Radiotherapy and Oncology 133 (2019) 100–105

Contents lists available at ScienceDirect

Radiotherapy and Oncology

journal homepage: www.thegreenjournal.com

Orignal Article

Applying a commercial atlas-based synthetic Computed Tomography algorithm to patients with hip prostheses for prostate Magnetic Resonance-only radiotherapy

Jonathan Wyatt *, Hazel McCallum

Northern Centre for Cancer Care, Newcastle Upon Tyne Hospitals NHS Foundation Trust, Newcastle, UK

ARTICLE INFO

Article history:
Received 21 August 2018
Received in revised form 24 December 2018
Accepted 30 December 2018
Available online 22 January 2019

Keywords:
MR-only radiotherapy planning
Magnetic Resonance imaging
Radiotherapy
Prostate
Hip prostheses

ABSTRACT

Background and purpose: Magnetic Resonance (MR)-only prostate radiotherapy has recently been clinically implemented using commercial synthetic Computed Tomography (sCT) algorithms. However patients with hip prostheses have been excluded from all MR-only research to date and assumed to require dedicated sCT algorithms. This study aimed to investigate the dosimetric accuracy of applying a commercial sCT algorithm, based on an atlas of patients without hip prostheses, to patients with prostheses.

Materials and methods: 18 patients with unilateral hip prostheses received MR and CT scans in the radiotherapy position. sCTs were generated from the MR using a commercial algorithm. The clinical Volumetric Modulated Arc Therapy (VMAT) plan, consisting of partial arcs which avoided the prosthesis, was recalculated using the sCT and the dose distribution compared.

Results: The mean isocentre dose difference was $\Delta D = (-0.4 \pm 0.2)\%$ (mean ± standard error of the mean (sem), range – 1.9%, 1.1%) and the mean differences in Planning Target Volume, bladder and rectum mean doses were ≤0.3%. The 3D global gamma pass rate with dose difference 1% and distance to agreement 1 mm within the body was $\Gamma^{1/1}_{Body} = (95.0 \pm 0.5)\%$ (sem) and within the 50% isodose volume, which excluded the prosthesis, was $\Gamma^{1/1}_{50\%} = (98.5 \pm 0.4)\%$ (sem). The pass rate within the PTV was $\Gamma^{2/2}_{PTV} \geq 99.7\%$ for all patients, although for PTVs close (≤3.5 cm) to the prosthesis $\Gamma^{1/1}_{PTV} < 85\%$ for three patients. The sCT did not accurately represent the prosthesis with a mean difference in radiological isocentre depth near the prosthesis of $\Delta d^{Rad}_{Outside} = (15.8 \pm 2.6)$ mm (sem). However inside the treatment plan arc the difference was $\Delta d^{Rad}_{Inside} = (-1.8 \pm 0.5)$ mm (sem).

Conclusions: Using a commercial prostate sCT algorithm for patients with unilateral hip prostheses is dosimetrically accurate (<0.5%) as long as the routine prosthesis-avoidance treatment planning approach is used and the PTV is >3.5 cm from the prosthesis. This suggests MR-only prostate radiotherapy can be extended to patients with hip prostheses without requiring a specific sCT algorithm.

© 2019 Elsevier B.V. All rights reserved. Radiotherapy and Oncology 133 (2019) 100–105

Magnetic Resonance (MR) imaging has an increasing role within prostate radiotherapy treatments due to its superior soft-tissue contrast for organ delineation compared to the routine Computed Tomography (CT) imaging [1]. The use of MR for prostate delineation has reduced prostate volumes [2] and lowered urinary frequency and urinary retention toxicity scores [3]. Typically the MR is registered with a CT, with the MR used for delineation and the CT for treatment planning because MR images cannot be calibrated for radiotherapy dose calculations. This MR-CT registration has an inherent uncertainty which impacts the entire patient's treatment [4]. This has motivated research into MR-only radiotherapy treatment planning which removes the registration uncertainty by replacing the CT with a synthetic CT (sCT) generated from the MR for dose calculations. MR-only radiotherapy is a rapidly developing field and is now being used clinically for the treatment of prostate cancer [5,6]. A large number of different sCT approaches have been reported in the literature, which can be classified into three categories: bulk density assignment, regression-based methods and atlas-based methods [7]. There are currently two commercially available solutions for the prostate clinical site, one using the atlas-based approach [8] and the other a bulk-density approach [9]. Both of these commercial sCTs have demonstrated dose differences <0.5% compared to doses calculated on CT [5,10].

The current MR-only literature has not considered patients with hip prostheses. All atlas-based approaches reported have used atlases constructed from patients without hip prostheses. This

* Corresponding author.
E-mail address: jonathanwyatt@nhs.net (J. Wyatt).

https://doi.org/10.1016/j.radonc.2018.12.029
0167-8140/© 2019 Elsevier B.V. All rights reserved.

has lead to the assumption that sCTs generated for patients with prostheses, or other unusual anatomy not present within the atlas, would be inaccurate [11]. Similarly the classification algorithm used within the commercial bulk-density approach has been trained using MR and CT data acquired on patients without hip prostheses [9] and patients with prostheses are automatically excluded [10]. The expectation has been that including hip prosthesis patients within an MR-only pathway would require specific sCT algorithms with atlases/classification models generated from hip prosthesis patients, entailing significant additional time and cost. This has lead clinical implementations to exclude hip prosthesis patients from MR-only pathways [6].

The number of hip replacement operations carried out in the UK has increased by over 50% in the last 10 years, with 101,651 patients operations carried out in 2016 [12,13]. This is likely to result in a corresponding increase in patients with hip prostheses requiring radiotherapy treatments. The presence of hip prostheses produces substantial artefacts in both MR and CT images. In MR images the hip prosthesis causes large susceptibility artefacts with significant geometric distortions surrounding the implant [14]. The MR artefacts are, however, localised to the implant and surrounding area and can be reduced using fast spin echo sequences with large receive bandwidths [15]. On CT the hip prosthesis causes large streak artefacts and photon starvation regions which can extend across the whole image [16]. MR has been shown to have benefits in prostate delineation compared to CT in patients without hip prostheses [17] and the more localised prosthesis artefacts on MR suggest it may also have additional delineation improvements for patients with prostheses. One small study found that MR images had reduced inter-observer variability compared to CT for prostate delineation in patients with bilateral hip prostheses [18]. Therefore it appears likely that patients with hip prostheses would also benefit from an MR-only radiotherapy approach and it is important to assess whether current sCT generation methods are accurate for prostate cancer patients with hip prostheses.

It is unlikely that sCT algorithms designed for patients without hip prostheses will accurately represent the hip prosthesis. However radiotherapy treatment planning in the presence of hip prostheses is also challenging due to dose calculation inaccuracies around the prosthesis in commercial treatment planning systems and the CT artefacts causing incorrect tissue densities to be determined [19]. Therefore radiotherapy treatment plans are typically designed to avoid beams entering through the prosthesis [20]. This means the inaccuracy of the sCT algorithm in the hip prosthesis region may not impact the sCT dosimetric accuracy as long as it is accurate in the rest of the image. If the sCT is dosimetrically accurate this will enable hip prosthesis patients to benefit from MR-only radiotherapy without the necessity of developing a specific algorithm for them. Therefore the aim of this study was to investigate the dosimetric accuracy of applying a commercial synthetic CT software containing an atlas of non-prosthesis patients to treat prostate cancer in patients with unilateral hip prostheses using the routine treatment planning approach that avoided the prosthesis.

Materials and methods

Patient data collection

18 patients with a unilateral hip prosthesis treated with radiotherapy for prostate cancer at the Northern Centre for Cancer Care (NCCC), Newcastle, UK were included in this retrospective, planning study. All radical prostate patients at the NCCC receive planning MR and CT scans, with a large field of view MR image routinely acquired. Patients were selected retrospectively from 677 patients treated with radical CT-based radiotherapy for prostate cancer between 1 September 2016 and 30 April 2018, with the following exclusion criteria (number of patients excluded): post-prostatectomy (1), MR not acquired (2), kilovoltage CT not acquired (1). Patients were diagnosed with prostate cancer (stages T2 to T4) with a median age of 74.5 years (range 65–82 years). All patient images were anonymised prior to inclusion in the study.

Patients received radiotherapy planning MR (1.5 T Magnetom Espree, Siemens, Erlangen, Germany) and CT (Sensation Open, Siemens, Erlangen, Germany) scans, performed on flat couch tops with local standard prostate radiotherapy immobilisation. Prior to each scan patients underwent routine bladder and bowel preparation. The bladder preparation protocol consisted of an empty bladder 30 minutes prior to the scan, followed by drinking 400 ml of water. The bowel preparation protocol required application of a micro-enema 45 minutes prior to the scan followed by bowel emptying. Internal fiducial markers were not present in any patient. The MR images were acquired using a 6 channel flexible receive coil (Siemens Body Matrix) supported over the patient by an in-house manufactured coil bridge and the 24 channel spine receive coil contained in the couch (Siemens Spine Matrix). This ensured the external patient contour was not deformed by the receive coils [21].

The MR images were acquired with a T2-weighted SPACE (Sampling Perfection with Application optimised Contrasts using different flip angle Evolution) sequence, a 3D turbo spin echo sequence. The acquisition parameters were previously optimised to produce geometrically robust images that encompassed the entire body contour [21] and are given in Table 1. Two patients were imaged with an older version of the protocol with a slightly larger voxel size of $1.8 \times 1.8 \times 1.7$ mm^3 but otherwise very similar parameters. The Siemens 3D distortion correction algorithm was applied to all images. The CT images were acquired with a voxel size of $1.1 \times 1.1 \times 3$ mm and a tube voltage of $V = 120$ kVp. No metal artefact reduction techniques were applied in either the CT or MR acquisition. Synthetic CTs were generated using MriPlanner (prostate model version 1.1.7, Spectronic Medical AB, Helsingborg, Sweden) [5,8]. A representative patient's planning CT, MR and sCT are shown in Fig. 1.

Treatment planning

All treatment planning was carried out using RayStation (version 7, RaySearch Laboratories, Stockholm, Sweden). The planning CT was rigidly registered to the MR using the automatic mutual information algorithm within RayStation. This is the clinical routine and the registration used in the study was the same registration used clinically. The sCT was in the same frame of reference as the MR, so the same registration matrix (planning CT-MR) was used with the sCT (planning CT-sCT). An external contour was automatically outlined on the CT and sCT using a Hounsfield Unit threshold of $T = -250$ HU. RayStation enables each imaging machine to have its own Hounsfield Unit to mass density calibration curve. Therefore the CT was calibrated using data measured

Table 1
The MR imaging protocol used.

Parameter	Value
Field of view/mm	450×450
Voxel size/mm^3	$1.4 \times 1.4 \times 1.5$
Number of slices	120
Repetition time/ms	1500
Echo time/ms	211
Flip angle/°	150
Bandwidth/HzPixel^{-1}	601
Echo train length	105
Echo spacing/ms	3.98

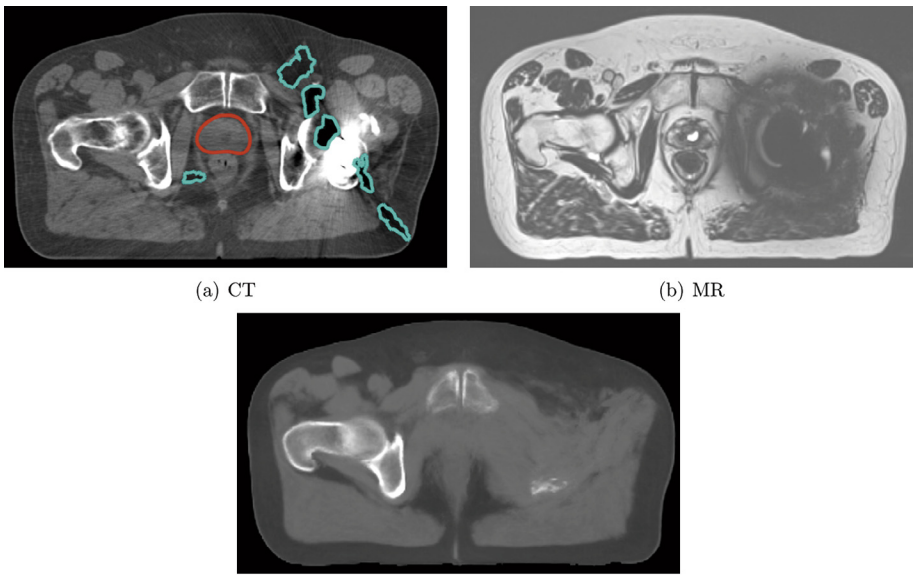

(a) CT (b) MR

(c) sCT

Fig. 1. CT (a), MR (b) and sCT (c) images for a representative patient. The hip prosthesis can be clearly seen in the CT image but just produces a signal void on the MR. The hip prosthesis produces artefacts across the whole image in the CT but only locally in the MR image. The over-ridden contour is shown on the CT in blue and the prostate contour in red. (For interpretation of the references to color in this figure legend, the reader is referred to the web version of this article.)

on the CT scanner and the sCT calibrated using data provided by Spectronic Medical AB (see Fig. S1 for the two calibration curves). The photon starvation artefacts from the prosthesis (but not the prosthesis itself) in the CT image were outlined and set to unit density. Any air in the rectum in the CT was set to unit density. Both of these contours were used clinically due to the lack of metal artefact reduction techniques on the CT scanner. The over-ridden contour is shown in Fig. 1.

The treatment plan used for the dosimetric comparison was the clinical plan used for patient treatment. This consisted of a 6 MV Volumetric Modulated Arc Therapy (VMAT) plan with one or two partial arcs which avoided entering through the hip prosthesis. For patients with left prostheses the arcs went from gantry angle G_{start} = 181° to G_{stop} = 10° (median, range G_{stop} = 350–15°). For right prosthesis patients the arcs went from G_{start} = 179° to G_{stop} = 350° (median, range G_{stop} = 5–310°). The prescription dose was 60 Gy in 20 fractions to 50% of the central Planning Target Volume (PTV) using the CHHiP trial planning protocol [22]. A $2 \times 2 \times 2$ mm^3 dose grid was used which covered the external contours of both CT and sCT. The treatment plan was recalculated on the sCT keeping the monitor units, the dose grid voxel size and the dose grid position the same.

Evaluation

The percentage difference in isocentre dose between the sCT and CT was calculated using

$$\Delta D = 100\frac{D_{sCT} - D_{CT}}{D_{CT}} \quad (1)$$

where D_{sCT} was the dose at the isocentre for the sCT and D_{CT} was the dose at the isocentre for the CT.

The differences in dose to the PTV Dose–Volume Histogram (DVH) points D2, D50, D98 and mean dose were calculated as a percentage of the prescription dose [23]. Similarly the differences in bladder DVH points D5, D25, D50 and mean dose, and rectum DVH points D3, D30, D60 and mean dose were calculated as a percentage of the prescription dose.

A gamma analysis was performed comparing the dose calculated on the CT to the sCT using the Medical Interactive Creative Environment (MICE) Toolkit (version 1.0.4, Umea University, Sweden) [24]. A 3D global gamma analysis was carried out within the following structures: the external contour, the PTV and the volume enclosed by the 50% isodose line. The gamma analysis criteria used were a dose difference of 1% of prescription dose (60 Gy) and distance to agreement 1 mm and dose difference 2% and distance to agreement 2 mm. All points below 10% of the prescription dose were excluded from the analysis.

The 6 MV radiological water equivalent isocentre depth was calculated at 5° angles for each image in the isocentre plane [8,25]. For the CT the radiological isocentre depth was calculated using density over-rides for the CT artefacts. For each patient the difference in radiological depth (CT – sCT) at each gantry angle was determined and the mean difference inside (within the start and stop gantry angles, see Fig. 2(c)) and outside the clinical VMAT arc calculated. The mean difference in radiological depth at each gantry angle was computed for the left prosthesis and right prosthesis patients separately. The physical isocentre depth at each gantry angle was also calculated as a measure of the difference in external contour between the scans (which can be seen in the gamma distribution in Fig. 2(c)), and the same analysis carried out. The minimum distance between the PTV and the prosthesis was also calculated for each patient using a distance transform function within RayStation.

Results

The dose distributions calculated on the sCT were similar to those calculated on the CT (see Fig. 2 for a typical patient), with a mean isocentre dose difference of $\Delta D = (-0.4 \pm 0.2)\%$ (mean ± standard error of the mean (sem), range −1.9%, 1.1%). The mean dose differences in PTV, bladder and rectum DVH points were similarly small (≤0.4%, see Table 2).

The gamma analysis showed good agreement between CT and sCT with a mean gamma pass rate within the external contour with gamma criteria 1%/1 mm of $\Gamma^{1/1}_{Body} = (95.0 \pm 0.5)\%$ (sem, range

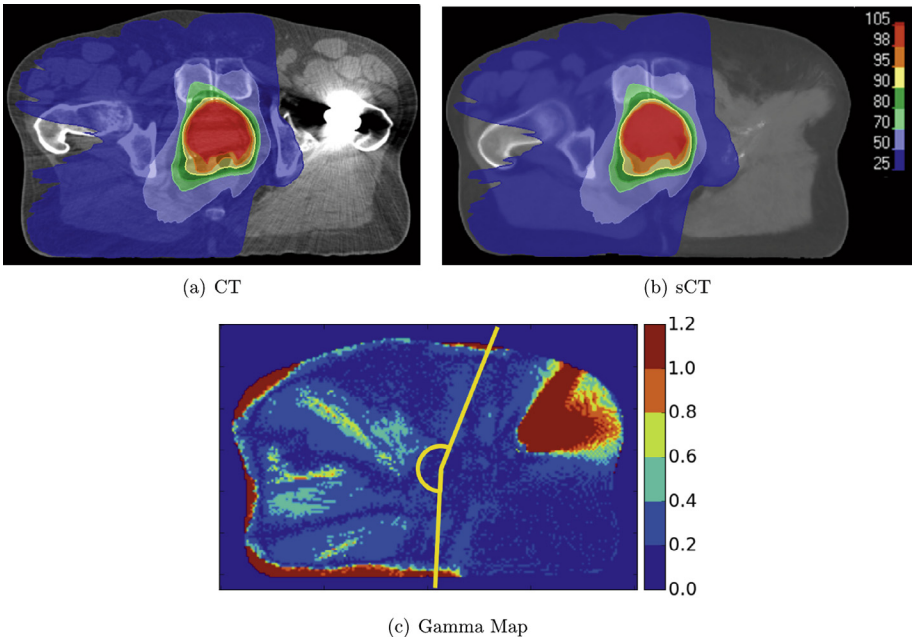

(a) CT (b) sCT

(c) Gamma Map

Fig. 2. Dose distributions on the CT (a) and sCT (b) for an example patient. The dose distribution is shown as % of the prescription dose. The gamma map with criteria1%/1 mm within the external contour for the same patient is also shown (c). The clinical plan avoids the hip prosthesis, with the VMAT arc shown in yellow. (For interpretation of the references to color in this figure legend, the reader is referred to the web version of this article.)

Table 2
The mean ± standard error of the mean (minimum, maximum) dose differences as a percentage of prescription dose for the PTV, bladder and rectum DVH points. Uncertainties are one standard error of the mean.

Structure	DVH parameter	Dose difference/%
PTV	D2	−0.2 ± 0.2 (−1.2, 0.8)
PTV	D50	−0.3 ± 0.1 (−1.0, 0.9)
PTV	D98	−0.4 ± 0.1 (−1.4, 0.9)
PTV	Mean	−0.3 ± 0.1 (−1.0, 0.9)
Bladder	D5	−0.3 ± 0.2 (−1.3, 1.0)
Bladder	D25	−0.1 ± 0.1 (−1.3, 1.0)
Bladder	D50	0.0 ± 0.1 (−1.0, 0.7)
Bladder	Mean	−0.1 ± 0.1 (−1.0, 0.7)
Rectum	D3	−0.3 ± 0.1 (−1.1, 1.0)
Rectum	D30	0.0 ± 0.1 (−0.8, 0.8)
Rectum	D60	0.0 ± 0.1 (−1.1, 1.3)
Rectum	Mean	−0.1 ± 0.1 (−0.6, 0.7)

90.9%–97.9%) and at 2%/ 2mm of $\Gamma^{2/2}_{Body}$ = (97.6 ± 0.3)% (94.5%–99.5%). This analysis included large dose differences within the prosthesis region which the sCT did not accurately reconstruct (see an example in Fig. 2). The gamma analysis within the 50% isodose volume, excluding the prosthesis region, gave improved results with mean pass rates $\Gamma^{1/1}_{50\%}$ = (98.5 ± 0.4)% (94.6%–100.0%) and $\Gamma^{2/2}_{50\%}$ = (99.98 ± 0.02)% (99.7%–100.0%). The mean gamma pass rate within the PTV was $\Gamma^{1/1}_{PTV}$ = (94.8 ± 1.8)% (74.8%–100.0%) and $\Gamma^{2/2}_{PTV}$ = (99.98 ± 0.01)% (98.9%–100.0%) for 1%/1 mm and 2%/2 mm respectively. The distribution of gamma passes can be seen in Fig. 3. There appeared to be some dependence of the gamma pass rate within the PTV on the minimum distance between the PTV and the prosthesis (see Fig. 3).

The mean difference in radiological isocentre depth outside the treatment plan arc, $\Delta d^{Rad}_{Outside}$ = (15.8 ± 2.6) mm (sem, range 1.2 mm–44.2 mm), was much greater than the mean difference inside the treatment plan arc, Δd^{Rad}_{Inside} = (−1.8 ± 0.5) mm (sem, range −7.5 mm–2.0 mm). In contrast the physical isocentre depth differences were similar inside and outside the treatment plan arc, Δd^{Phys}_{Inside} = (1.0 ± 0.2) mm (sem, range − 0.9 mm–2.8 mm) and $\Delta d^{Phys}_{Outside}$ = (−0.3 ± 0.3) mm (sem, range 2.8 mm–1.7 mm). The radiological isocentre depths as a function of gantry angle shows small differences (<6 mm) inside the clinical treatment plan (see Fig. 4).

Discussion

This study has evaluated the dosimetric accuracy of applying a commercial atlas-based prostate sCT algorithm to patients with unilateral hip prostheses utilising a prosthesis avoidance planning approach. Overall the dosimetric differences between sCT and CT were small, with the mean isocentre dose difference and DVH differences being ≤0.4%. As expected, the sCT algorithm did not accurately represent the prosthesis, leading to very large differences in radiological depth for that region. However, because the routine clinical treatment planning approach was to avoid entering through the prosthesis region (see Fig. 4), this difference in radiological depth made very little difference to the dose distribution in the high dose region. This can be seen by the small mean difference in radiological depth within the VMAT arc. This is also shown by the high gamma pass rates within the 50% isodose region (which avoids the prosthesis) with a minimum pass rate of $\Gamma^{1/1}_{50\%}$ = 94.6% at 1%/1 mm and $\Gamma^{2/2}_{50\%}$ = 99.7% at 2%/2 mm.

However the gamma pass rates for the PTV at 1%/1 mm for some patients were substantially lower, with three patients having pass rates <85%. The PTV gamma pass rate appeared to show some dependence on the minimum distance from the PTV to the implant, with all pass rates 92% occurring in patients with the minimum PTV-implant distance ≤3.5 cm (see Fig. 3). Visual inspection showed that the gamma fails in these patients occurred in the prosthesis side of the PTV. This suggests that the sCT algorithm may not provide sufficient dosimetric accuracy for PTV's close (≤3.5 cm) to the prosthesis. However another important consideration is the accuracy of the dose calculated on CT in regions adjacent to the prosthesis. The prostheses produced substantial CT

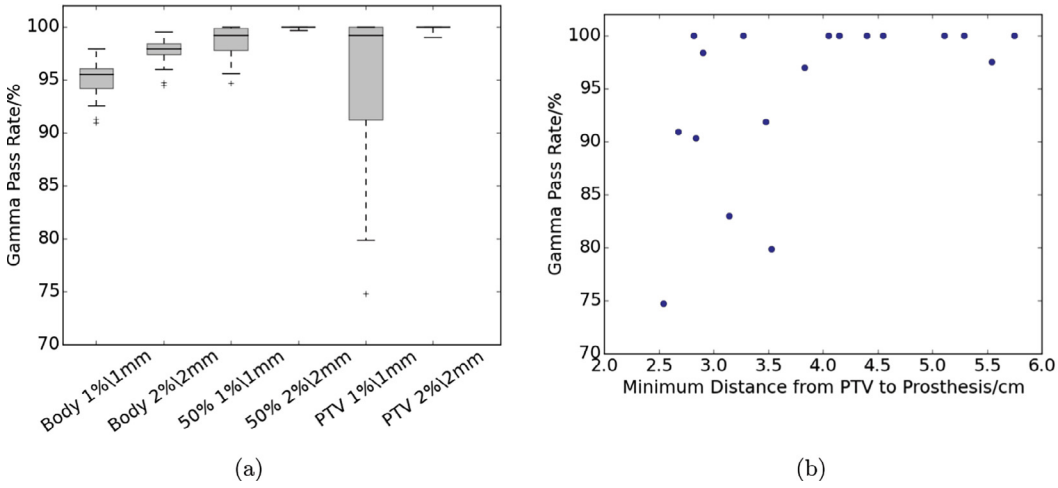

Fig. 3. The distribution of gamma pass rates with different gamma criteria and masking structures (a) and the gamma pass rate within the PTV as a function of the minimum distance between the PTV and the prosthesis (b). Masking structure 50% refers to the 50% isodose contour. The gamma criteria used in (b) was dose difference 1% and distance to agreement 1 mm.

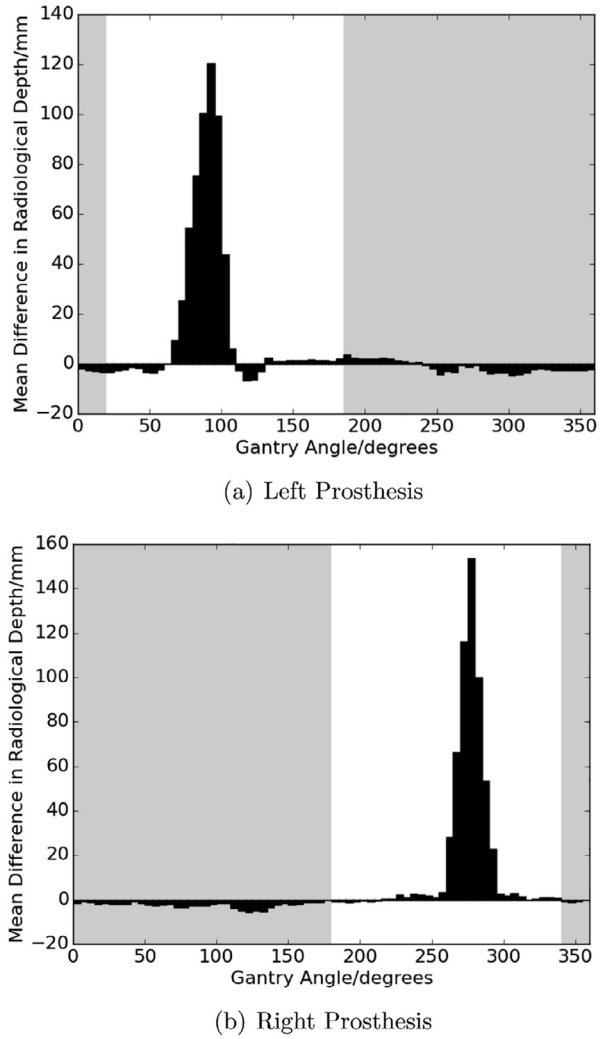

Fig. 4. The mean difference in radiological depth at each gantry angle for left prosthesis patients (a) and right prosthesis patients (b). The shaded area indicates the maximum range of gantry angles used in the clinical VMAT arcs.

artefacts which were manually outlined and set to unit density (water) on the planning system. This process may not have accurately represented the patient anatomy which could be contributing to the dose differences observed for these patients. Future work could investigate this by acquiring CTs with recently developed commercial metal artefact reduction techniques [26] to improve the gold standard CT the sCT is compared to. A final consideration of the observed low gamma pass rates within the PTV for these three patients is that the dose differences were still relatively small, with the gamma pass rates at 2%/2 mm being 99.7% for one patients and 100.0% for all 17 other patients. Therefore it is likely that the dose differences for these patients would still be considered clinically acceptable.

To the author's knowledge no other study in the literature has investigated the dosimetric accuracy of synthetic CTs for patients with hip prostheses. The dosimetric results from this study were similar to those reported using the same sCT algorithm on patients without hip prostheses [5]. The DVH dose differences were all <0.3% which compared well with the 0.4% found in this prosthesis study. The mean dose differences in PTV, bladder and rectum mean doses all agreed within one standard error of the mean and the range of dose differences in mean organ dose in this study (−1.0% to 0.9%), was contained within the range reported in the non-prosthesis study (−1.15% to 1.42%). This suggests that the sCT algorithm has a similar level of dosimetric accuracy for patients with hip prostheses as for patients without. The mean dose differences in DVH points was also similar to the ≤0.5% reported from the other commercially available sCT algorithm [10], as well as within the 0.3–2.0% range of dose differences reported within the literature [27].

This study has suggested that a sCT algorithm designed for patients without hip prostheses can be used for prostheses patients with a similar dosimetric uncertainty. This is a small increase in dosimetric uncertainty compared to a MR-CT planning process, but the MR-only planning approach has the advantage of reduced geometrical uncertainty through removing the MR-CT registration and its associated uncertainty. The dosimetric uncertainty of the complete radiotherapy process is recommended to be within 3% and the geometric uncertainty to be 2–4 mm, which requires the uncertainty of any component of the radiotherapy pathway to be ≤1% and ≤1 mm [28]. The mean dose difference reported here was 0.4% and the estimated MR-CT registration uncertainty for the prostate is 2 mm [4]. This suggests that a MR-only planning technique using this commercial atlas-based sCT algorithm will improve the overall radiotherapy accuracy for patients with hip

prostheses. Using a standard sCT algorithm for hip prosthesis patients will simplify MR-only workflows and enable prosthesis patients to benefit from MR-only radiotherapy without the requirement for specific algorithms to be developed.

Future work will investigate the feasibility of treatment plan design and optimisation using the sCT, in particular determining the start and stop angles of the treatment, and validate the algorithm on a larger patient cohort. Successfully demonstrating this will enable clinical implementation of MR-only planning for prostate patients with unilateral hip prostheses utilising a standard prostate sCT algorithm.

In conclusion, the dosimetric accuracy of a commercial prostate sCT algorithm for patients with unilateral hip prosthesis appears to be similar to the dosimetric accuracy of patients without prostheses, with mean dose differences $\leq$0.4% when using a VMAT prosthesis-avoidance planning approach. This study suggests that using a standard sCT algorithm is a promising approach for including patients with hip prostheses within MR-only pathways.

Acknowledgements

The authors acknowledge the access to the MriPlanner software provided through a research collaboration with Spectronic Medical AB.

Conflicts of interest

The authors have no conflicts of interest to declare.

Appendix A. Supplementary data

Supplementary data to this article can be found online at https://doi.org/10.1016/j.radonc.2018.12.029.

References

[1] Khoo V, Joon D. New developments in MRI for target volume delineation in radiotherapy. Br J Radiol 2006;79:s2–S15.
[2] Rasch C, Barillot I, Remeijer P, Touw A, van Herk M, Lebesque JV. Definition of the prostate in CT and MRI: a multi-observer study. Int J Radiat Oncol Biol Phys 1999;43:57–66.
[3] Sander L, Langkilde NC, Holmberg M, Carl J. MRI target delineation may reduce long-term toxicity after prostate radiotherapy. Acta Oncol 2014;53:809–14.
[4] Nyholm T, Nyberg M, Karlsson MG, Karlsson M. Systematisation of spatial uncer- tainties for comparison between a MR and a CT-based radiotherapy workflow for prostate treatments. Radiat Oncol 2009;4:1.
[5] Persson E, Gustafsson C, Nordström F, Sohlin M, Gunnlaugsson A, Petruson K, Rintelä N, Hed K, Blomqvist L, Zackrisson B, et al. MR-OPERA–a multi-center/multi- vendor validation of MRI-only prostate treatment planning using synthetic CT images. Int J Radiat Oncol Biol Phys 2017;99:692–700.
[6] Tenhunen M, Korhonen J, Kapanen M, Seppälä T, Koivula L, Collan J, Saarilahti K, Visapää H. MRI-only based radiation therapy of prostate cancer: workflow and early clinical experience. Acta Oncol 2018;57:902–7.
[7] Johnstone E, Wyatt JJ, Henry AM, Short SC, Sebag-Montefiore D, Murray L, et al. A systematic review of synthetic computed tomography generation methodologies for use in magnetic resonance imaging – only radiation therapy. Int J Radiat Oncol Biol Phys 2018;100:199–217.
[8] Siversson C, Nordström F, Nilsson T, Nyholm T, Jonsson J, Gunnlaugsson A, Olsson LE. Technical note: MRI only prostate radiotherapy planning using the statistical decomposition algorithm. Med Phys 2015;42:6090–7.
[9] Köhler M, Vaara T, Grootel M, Hoogeveen R, Kemppainen R, Renisch S. MR-only simulation for radiotherapy planning. Philips White Paper 2015.
[10] Tyagi N, Fontenla S, Zhang J, Cloutier M, Kadbi M, Mechalakos J, et al. Dosimetric and workflow evaluation of first commercial synthetic CT software for clinical use in pelvis. Phys Med Biol 2017;62:2961.
[11] Dowling JA, Sun J, Pichler P, Rivest-Ḥenault D, Ghose S, Richardson H, Wratten C, Martin J, Arm J, Best L, et al. Automatic substitute computed tomography generation and contouring for magnetic resonance imaging (MRI)-alone external beam radiation therapy from standard MRI sequences. Int J Radiat Oncol Biol Phys 2015;93:1144–53.
[12] National Joint Register 4th Annual Report, 2007.
[13] National Joint Register 14th Annual Report, 2017.
[14] Koch K, Hargreaves B, Pauly KB, Chen W, Gold G, King K. Magnetic resonance imaging near metal implants. J Magn Reson Imaging 2010;32:773–87.
[15] McRobbie DW, Moore EA, Graves MJ. MRI from picture to proton. Cambridge University Press; 2017.
[16] Barrett JF, Keat N. Artifacts in CT: recognition and avoidance. Radiographics 2004;24:1679–91.
[17] Dubois DF, Prestidge BR, Hotchkiss LA, Prete JJ, Bice Jr WS. Intraobserver and interobserver variability of MR imaging-and CT-derived prostate volumes after transperineal interstitial permanent prostate brachytherapy. Radiology 1998;207:785–9.
[18] Rosewall T, Kong V, Vesprini D, Catton C, Chung P, Ḿenard C, Bayley A. Prostate delineation using CT and MRI for radiotherapy patients with bilateral hip prostheses. Radiother Oncol 2009;90:325–30.
[19] Ng WL, Brunt J, Temple S, Saipillai M, Haridass A, Wong H, et al. Volumetric modulated arc therapy in prostate cancer patients with metallic hip prostheses in a UK centre. Rep Pract Oncol Radiother 2015;20:273–7.
[20] Reft C, Alecu R, Das IJ, Gerbi BJ, Keall P, Lief E, et al. Dosimetric considerations for patients with HIP prostheses under- going pelvic irradiation. Report of the AAPM radiation therapy committee task group 63. Med Phys 2003;30:1162–82.
[21] Paulson ES, Erickson B, Schultz C, Li XA. Comprehensive MRI simulation method- ology using a dedicated MRI scanner in radiation oncology for external beam radiation treatment planning. Med Phys 2015;42:28–39.
[22] Dearnaley D, Syndikus I, Mossop H, Khoo V, Birtle A, Bloomfield D, et al. Conventional versus hypofractionated high-dose intensity-modulated radiotherapy for prostate cancer: 5-year outcomes of the randomised, non-inferiority, phase 3 CHHiP trial. Lancet Oncol 2016;17:1047–60.
[23] Gŕegoire V, Mackie T, De Neve W, Gospodarowicz M, Purdy J, van Herk M, Niemierko A. State of the art on dose prescription, reporting and recording in intensity- modulated radiation therapy (icru report no. 83). Cancer Radiother 2011;15:555–9.
[24] Nyholm T, Berglund M, Brynolfsson P, Jonsson J. EP-1533: ICE-studio-an interactive visual research tool for image analysis. Radiother Oncol 2015;115: S837.
[25] Maspero M, Seevinck P, Schubert G, Hoesl M, van Asselen B, Viergever M, Lagendijk J, Meijer G, van den Berg C. Quantification of confounding factors in mri-based dose calculations as applied to prostate IMRT. Phys Med Biol 2017;62.
[26] Andersson KM, Nowik P, Persliden J, Thunberg P, Norrman E. Metal artefact reduction in CT imaging of hip prostheses: an evaluation of commercial techniques provided by four vendors. Br J Radiol 2015;88:20140473.
[27] Edmund JM, Nyholm T. A review of substitute CT generation for MRI-only radiation therapy. Radiat Oncol 2017;12:28.
[28] Thwaites D. Accuracy required and achievable in radiotherapy dosimetry: have modern technology and techniques changed our views? J Phys Conf Ser 2013;444:012006.